13. N. Balakrishnan, A. Dalgarno, *Chem. Phys. Lett.* **341**, 652 (2001).
14. E. Bodo, F. A. Gianturco, A. Dalgarno, *J. Chem. Phys.* **116**, 9222 (2002).
15. D. W. Chandler, *J. Chem. Phys.* **132**, 110901 (2010).
16. P. F. Weck, N. Balakrishnan, *J. Chem. Phys.* **122**, 154309 (2005).
17. G. Quéméner, N. Balakrishnan, B. K. Kendrick, *J. Chem. Phys.* **129**, 224309 (2008).
18. B. Brutschy, H. Haberland, K. Schmidt, *J. Phys. B* **9**, 2693 (1976).
19. Q. Wei, I. Lyuksyutov, D. Herschbach, *J. Chem. Phys.* **137**, 054202 (2012).
20. L. Boltzmann, *Vorlesung Uber Gastheorie II* (J. A. Barth, Leipzig, Germany, 1989).
21. D. L. Bunker, N. Davidson, *J. Am. Chem. Soc.* **80**, 5085 (1958).
22. A. Schutte, D. Bassi, F. Tommasini, G. Scoles, *Phys. Rev. Lett.* **29**, 979 (1972).
23. J. P. Toennies, W. Welz, G. Wolf, *J. Chem. Phys.* **61**, 2461 (1974).
24. J. P. Toennies, W. Welz, G. Wolf, *J. Chem. Phys.* **71**, 614 (1979).
25. Ch. Buggle, J. Léonard, W. von Klitzing, J. T. M. Walraven, *Phys. Rev. Lett.* **93**, 173202 (2004).
26. N. R. Thomas, N. Kjaergaard, P. S. Julienne, A. C. Wilson, *Phys. Rev. Lett.* **93**, 173201 (2004).
27. S. Chefdeville *et al.*, *Phys. Rev. Lett.* **109**, 023201 (2012).
28. E. P. Wigner, *Phys. Rev.* **73**, 1002 (1948).
29. J. M. Doyle, B. Friedrich, J. Kim, D. Patterson, *Phys. Rev. A* **52**, R2515 (1995).
30. C. D. Ball, F. C. De Lucia, *Phys. Rev. Lett.* **81**, 305 (1998).
31. B. R. Rowe, G. Dupeyrat, J. B. Marquette, P. Gaucherel, *J. Chem. Phys.* **80**, 4915 (1984).
32. I. W. M. Smith, *Angew. Chem. Int. Ed.* **45**, 2842 (2006).
33. Y. T. Lee, J. D. Mcdonald, P. R. Lebreton, D. Herschbach, *Rev. Sci. Instrum.* **40**, 1402 (1969).
34. C. Berteloite *et al.*, *Phys. Rev. Lett.* **105**, 203201 (2010).
35. J. J. Gilijamse, S. Hoekstra, S. Y. T. van de Meerakker, G. C. Groenenboom, G. Meijer, *Science* **313**, 1617 (2006).
36. L. P. Parazzoli, N. J. Fitch, P. S. Żuchowski, J. M. Hutson, H. J. Lewandowski, *Phys. Rev. Lett.* **106**, 193201 (2011).
37. B. C. Sawyer, B. K. Stuhl, D. Wang, M. Yeo, J. Ye, *Phys. Rev. Lett.* **101**, 203203 (2008).
38. B. C. Sawyer *et al.*, *Phys. Chem. Chem. Phys.* **13**, 19059 (2011).
39. R. H. Neynaber, in *Advances in Atomic and Molecular Physics*, D. R. Bates, E. Immanuel, Eds. (Academic Press, New York, 1969), vol. 5, pp. 57–108.
40. P. E. Siska, *Rev. Mod. Phys.* **65**, 337 (1993).
41. U. Even, J. Jortner, D. Noy, N. Lavie, C. Cossart-Magos, *J. Chem. Phys.* **112**, 8068 (2000).
42. K. Luria, N. Lavie, U. Even, *Rev. Sci. Instrum.* **80**, 104102 (2009).
43. S. Burdenski, R. Feltgen, F. Lichterfeld, H. Pauly, *Chem. Phys. Lett.* **78**, 296 (1981).
44. D. W. Martin, C. Weiser, R. F. Sperlein, D. L. Bernfeld, P. E. Siska, *J. Chem. Phys.* **90**, 1564 (1989).
45. K. T. Tang, J. P. Toennies, *J. Chem. Phys.* **80**, 3726 (1984).
46. D. T. Colbert, W. H. Miller, *J. Chem. Phys.* **96**, 1982 (1992).
47. N. Moiseyev, *Non-Hermitian Quantum Mechanics* (Cambridge Univ. Press, Cambridge, 2011).
48. F. Lique, G. Li, H. -J. Werner, M. H. Alexander, *J. Chem. Phys.* **134**, 231101 (2011).

Acknowledgments: We acknowledge U. Even for many helpful discussions and sound advice. We thank R. Ozeri for most fruitful discussions; M. Raizen, R. Naaman, Y. Prior, and B. Dayan for a careful reading of the manuscript; and S. Assayag and M. Vinetsky from the Weizmann machine shop for assistance in designing and manufacturing of our vacuum chamber. This research was made possible, in part, by the historic generosity of the Harold Perlman Family. E.N. acknowledges support from the Israel Science Foundation and Minerva Foundation.

2 July 2012; accepted 6 September 2012
10.1126/science.1229141

An Ancient Core Dynamo in Asteroid Vesta

Roger R. Fu,[1]* Benjamin P. Weiss,[1] David L. Shuster,[2,3] Jérôme Gattacceca,[4] Timothy L. Grove,[1] Clément Suavet,[1] Eduardo A. Lima,[1] Luyao Li,[1] Aaron T. Kuan[5]

The asteroid Vesta is the smallest known planetary body that has experienced large-scale igneous differentiation. However, it has been previously uncertain whether Vesta and similarly sized planetesimals formed advecting metallic cores and dynamo magnetic fields. Here we show that remanent magnetization in the eucrite meteorite Allan Hills A81001 formed during cooling on Vesta 3.69 billion years ago in a surface magnetic field of at least 2 microteslas. This field most likely originated from crustal remanence produced by an earlier dynamo, suggesting that Vesta formed an advecting liquid metallic core. Furthermore, the inferred present-day crustal fields can account for the lack of solar wind ion-generated space weathering effects on Vesta.

The terrestrial planets are thought to have formed from the successive growth and accretion of protoplanetary objects <1000 km in diameter (*1*). A fraction of these protoplanets have survived to the present day and include 4 Vesta, the second most massive asteroid (525 km mean diameter). In particular, Vesta's high density, primordial basaltic crust, and large size suggest that it is an intact remnant of the early solar system that escaped catastrophic collisional disruption (*2*). Vesta therefore provides an opportunity to characterize the building blocks of the terrestrial planets and to study the processes of planetesimal accretion and differentiation.

Meteorites of the howardite-eucrite-diogenite (HED) clan probably sample the crust and upper mantle of Vesta (*3*). Geochemical studies of HED meteorites suggest that Vesta has a fully differentiated structure, with a metallic core ranging from 5 to 25% of the total planetary mass (*4*) that formed within ~1 to 4 million years (My) of the beginning of the solar system (*5, 6*). Recent volume and mass constraints from the NASA Dawn mission provide evidence of a metallic core between 107 and 113 km in radius (*2*).

Vigorous advection in a molten metallic core may generate a dynamo magnetic field. Paleomagnetic studies of meteorites suggest that past dynamos may have existed on other asteroidal objects such as the angrite and the CV carbonaceous chondrite parent bodies (*7, 8*). These data offer the possibility of studying the physics of dynamo action in a small-body regime not represented by active dynamos in the solar system today, in which Mercury is the smallest body with a known active dynamo (*9*). However, there has been no meteorite group for which evidence of dynamo action has been confidently established and that has been directly associated with a known, intact, asteroidal parent body.

Previous paleomagnetic studies have shown that many HED meteorites are low-fidelity recorders of magnetic fields because of their large (i.e., multidomain), low-coercivity magnetic minerals (*10*). Furthermore, these paleomagnetic studies generally lacked radiometric ages and thermochronometry. As a result, they came to no firm conclusions about the origin of magnetization identified in HED meteorites (*11*). Although dynamo-generated and even nebular fields were considered, other potential sources such as recent magnetic contamination and impact-generated fields could not be ruled out (*10, 12–14*). Here, we present a paleomagnetic study of ALHA81001 (ALH, Allan Hills), a meteorite found in Antarctica in 1981 with exceptional magnetic recording properties (*15*). We also present thermochronologic and petrographic data that constrain the origin of the meteorite's natural remanent magnetization (NRM).

The main–HED-group oxygen isotopic composition of ALHA81001 suggests that it originated on Vesta (*16*). As a eucrite, ALHA81001 has a basaltic composition and probably is a sample of the asteroid's upper crust. Our petrographic observations show that ~99 volume % of ALHA81001 has a fine-grained texture. A previous paleomagnetic study found that ALHA81001 has one of the most stable NRM records observed for any main–oxygen-isotope group HED

[1]Department of Earth, Atmospheric, and Planetary Sciences, Massachusetts Institute of Technology, 77 Massachusetts Avenue, Cambridge, MA 02139, USA. [2]Department of Earth and Planetary Science, University of California, Berkeley, CA 94720, USA. [3]Berkeley Geochronology Center, 2455 Ridge Road, Berkeley, CA 94709, USA. [4]Centre Européen de Recherche et d'Enseignement des Géosciences de l'Environnement, CNRS/Université Aix-Marseille 3, France. [5]Department of Applied Physics, Harvard University, Cambridge, MA 02138, USA.

*To whom correspondence should be addressed. E-mail: rogerfu@mit.edu

(*10*). This is probably due to its very fine grain size, which has led to the formation of unusually high-coercivity ferromagnetic crystals [kamacite and iron sulfide (*17*)]. In particular, the width of plagioclase phenocrysts in the groundmass ALHA81001 indicates that the primary crystallization of the meteorite above 1150°C took place over the course of ~1 hour (*18*). However, the presence of ~0.4-μm-wide augite exsolution lamellae in host pigeonite grains suggests that the meteorite was reheated to between 800° and 1100°C, possibly due to burial in a hot ejecta blanket, and then cooled slowly over several hundred years (*19*). Because these temperatures are above the Curie point of FeNi minerals, any remanent magnetization in ALHA81001 must have been acquired during or after this slow-cooling episode. Furthermore, we observed no undulatory extinction in plagioclase phenocrysts in the groundmass (*20*), indicating that the meteorite escaped impact shock pressures above 5 GPa after this slow cooling (*21*).

We extracted 13 subsamples (a set of 9 and a second set of 4) from two parent samples of ALHA81001. The subsamples within the first and second sets were mutually oriented to within 5° and 10°, respectively, whereas the two parent pieces were not mutually oriented. Subsamples taken from near the fusion crust produced by atmospheric passage have systematically different NRM directions from those of seven interior subsamples, whereas two subsamples extracted from between the fusion crust and the interior subsamples have intermediate NRM directions (Fig. 1). These data are consistent with heating and remagnetization of the meteorite's <2-mm-deep exterior during atmospheric passage and suggest that the interior was not strongly contaminated by hand magnets, weathering, or viscous remagnetization since the samples' arrival on Earth.

All 13 subsamples were progressively alternating field (AF) demagnetized or thermally demagnetized to characterize their NRM components. We observed three distinct components of magnetization in each subsample (Figs. 1, 2), with the exception of one fusion-crusted subsample, which has only two components. A low-coercivity (LC) component is blocked up to a coercivity of 3 mT. Its unidirectionality across all subsamples and low coercivity are consistent with a viscous remanent magnetization (VRM) acquired since the meteorite's recovery from Antarctica in 1981. A medium-coercivity (MC) and medium blocking temperature (MT) component, blocked from 3 to between 21 and 57 mT during AF demagnetization and up to 150°C during thermal demagnetization, is unidirectional across all subsamples (except one fusion-crusted subsample that does not have an MC component). Its low blocking temperature and unidirectionality across all subsamples strongly suggest that it is a VRM acquired during the meteorite's residence in Antarctica. The intensities of both the LC and MC/MT components are also consistent with a VRM origin according to our laboratory VRM-acquisition experiments (*22*).

Fusion-crusted and interior subsamples each carry distinct high-coercivity components (which we designate HCf and HC, respectively) that are blocked between 21 to 57 mT and 62 to >290 mT. The HC component is unidirectional throughout the interior subsamples (which are separated by up to 0.9 cm), and the HCf component is unidirectional across the fusion-crusted subsamples, but the HC and HCf directions are mutually divergent (Fig. 1). Thermal demagnetization identified a high-temperature (HT) magnetization in the same direction as the HC component and blocked between 150° and >275°C, above which irreversible alteration of the magnetization carriers occurs (*23*).

Upon AF demagnetization, the HC magnetization decays linearly to the origin with remarkable stability as compared to the NRM observed in all previously measured HED meteorites (*10, 12*) (Fig. 2). Its AF demagnetization spectrum is most similar to that of an anhysteretic remanent magnetization (ARM) and differs from that of a strong field (280 mT) isothermal remanent magnetization (IRM) or pressure remanent magnetization (PRM) acquired in a laboratory field of 750 μT at a pressure of up to 1.8 GPa [an analog for shock remanent magnetization (SRM) (*22*)]. All of these characteristics suggest that the HC/HT component is a thermoremanent magnetization (TRM) acquired during cooling in a magnetic field (*24*).

The $^{40}Ar/^{39}Ar$ plateau age of ALHA81001 indicates that the most recent heating event capable of full thermal remagnetization took place at 3.69 billion years ago (Ga) (Fig. 3C) and that the meteorite has largely escaped subsequent thermal disturbances. In particular, the observed degassing of radiogenic ^{40}Ar can be accounted for by a mean effective temperature between –50° and 140°C during the past 15 My (i.e., during transfer to Earth; see Fig. 3D). This is entirely consistent with our ^{38}Ar analysis, which reveals a cosmic ray exposure age of ~15 My, during which time the meteoroid may have been heated to a constant temperature of no more than 140°C (Fig. 3A). Blocking temperature relationships for kamacite and pyrrhotite (*25, 26*) and the degree of post–3.69 Ga heating inferred from ^{40}Ar and ^{38}Ar diffusion suggest that the HC/HT component should have survived from 3.69 Ga to the present day.

Our ARM and IRM paleointensity experiments indicate that the magnetizing field that produced the HC/HT component at 3.69 Ga most likely had

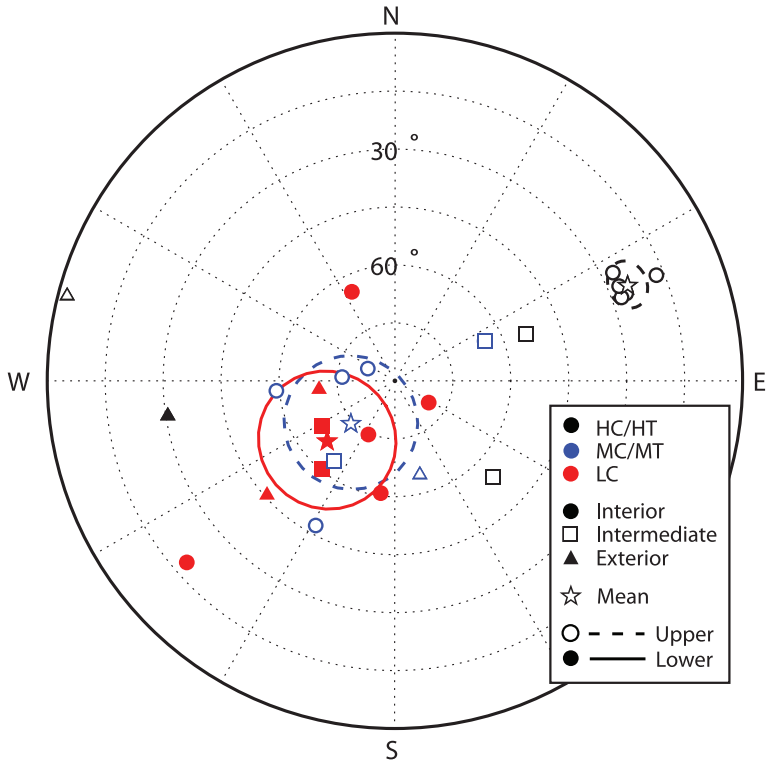

Fig. 1. NRM directions in eucrite ALHA81001. This is an equal-area stereographic projection showing the three components of magnetization observed in each subsample as inferred from principal components analyses. Black, blue, and red symbols represent HC/HT, MC/MT, and LC directions, respectively. Stars indicate average directions for each component. Dashed circles denote the 95% confidence interval for the true direction of magnetization assuming a Fisher distribution in the upper hemisphere, and solid circles denote it in the lower hemisphere. Exterior fusion-crusted subsamples, intermediate-depth subsamples (depth from surface between 0.7 and 2.0 mm), and interior subsamples (depth >2 mm) are shown by triangles, squares, and circles, respectively. Open symbols represent the upper hemisphere; solid symbols represent the lower hemisphere.

an intensity of ~12 μT (with a minimum value of ~2 μT) (*27*). The young $^{40}Ar/^{39}Ar$ age of ALHA81001 precludes the direct recording of a dynamo, because the longest predicted duration of a dynamo for a Vesta-sized object is on the order of several tens of millions of years to ~100 My after solar system formation (*28, 29*). Likewise, solar and nebular fields could not be a source of the magnetization, because they should have dissipated within the first ~6 My of solar system formation (*30*). Furthermore, slow cooling of ALHA81001 over $>10^2$ years rules out the recording of any putative transient, impact-generated fields, which are expected to have persisted for less than several hundred seconds under Vestan impact conditions (*31*). This leaves remanent magnetization of the Vestan crust and underlying materials as the most likely magnetic field source. This in turn requires that the crust was magnetized by an earlier ambient magnetic field. Given the high inferred paleointensities for ALHA81001, this earlier magnetic field was most likely due to a core dynamo. Although nebular fields may have had intensities comparable to those of core dynamos (*32*), they should have existed only during the first <6 My after solar system formation and typically varied in direction on time scales of several tens of orbits. Petrographic studies show that Vesta's crust cooled from the 780°C Curie point of kamacite to ambient space temperatures over at least several million years and therefore is unlikely to have coherently recorded such time-variable nebular fields (*33*). Another possibility is that Vesta's crust near or antipodal to large impact basins may have acquired remanent magnetization due to transient, impact-generated magnetic fields (*34, 35*). However, the low velocities (~5 km/s) expected for impacts on Vesta should not have typically produced the ionized plasma clouds necessary for generating strong transient magnetic fields (*36–38*). On the other hand, an early dynamo field should have been capable of generating steady core magnetic fields with intensities up to 2600 μT, resulting in surface fields of up to the order of 100 μT assuming a dominantly dipolar field geometry (*13, 39*), thereby providing a means of magnetizing the Vestan crust and underlying material.

Following (*40*), we calculated the expected strength of the remanent crustal field due to this earlier dynamo. Although most HED meteorites exhibit saturation remanence of between 10^{-4} and 10^{-2} A·m^2 kg^{-1} (*41*), certain previously unmeasured metal-rich HEDs may have higher values. We measured the saturation remanence of one such HED meteorite, Camel Donga, to be 5×10^{-2} A·m^2 kg^{-1} (*31*). Using this value for saturation remanence, a 100-μT field is expected to impart a TRM of intensity M_{TRM} up to 3×10^{-6} to 2×10^{-3} A·m^2 kg^{-1} in HED material (*42*). The resulting magnetic fields generated by a crust magnetized to these values depend on the specific geometry of the magnetized material. We calculated the expected field for one plausible geometry. Because ALHA81001 is probably an impact melt (*43*), we evaluated the magnetic field within an impact-heated region in a thin crust magnetized perpendicular to the plane (*31*). The resulting field is $\sim 2/3\mu_0 M_{TRM}\rho$, where μ_0 is the permeability of free space and ρ is the crustal density, assumed to be 3000 kg m^{-3}. Crustal material on Vesta magnetized in a dynamo with this geometry can therefore generate magnetic field intensities between 0.01 and ~4 μT.

Although the upper end of this range agrees with our inferred paleointensities, our paleointensities are nevertheless surprisingly high and may suggest the presence of more strongly magnetic material on or beneath the surface of Vesta that is not sampled by HED meteorites. Carbonaceous chondrite material has been observed in howardites and may have been observed as localized dark terrains on the surface of Vesta (*44*). Mesosiderites have been hypothesized to originate on Vesta because of the similarity of their oxygen isotopic compositions to those of HEDs (*45*). Carbonaceous chondrites and mesosiderites have saturation remanence values in excess of 10^{-1} A·m^2 kg^{-1} (*41*) and therefore can readily produce >10-μT crustal magnetic fields when magnetized in a 100-μT dynamo field. Therefore, such material, if present on Vesta, may result in localized, highly magnetic terrains. The high paleointensity of ALHA81001, which is stronger than that of most previously studied HEDs (*10*), may attest to the relative rarity of the purported highly magnetic terrains. Localized regions of high crustal field intensities on Mars and the Moon are similarly too intense to be explained by the observed magnetism of known martian meteorites and Apollo samples, respectively, and also require the existence of unsampled, highly magnetic material on these bodies (*40, 46*). A magnetized crust due to a prior dynamo epoch therefore appears to be the only plausible field-generation mechanism consistent with our inferred paleointensities.

Our inferred detection of an early dynamo in Vesta provides further evidence that dynamos could have formed in small differentiated bodies in the early solar system. The presence of a magnetized crust implies that at least parts of the Vestan surface had solidified and cooled below the Curie temperature during the presence of an active dynamo. The strong inferred intensity of remanent crustal magnetization suggests that the dynamo, when it was active, probably generated surface fields with intensities between 10 and 100 μT and that strongly magnetic material unsampled by HED meteorites may be present on or below the surface of Vesta. Furthermore, the existence of crustal magnetization at 3.69 Ga suggests that Vesta is likely to have crustal magnetic fields at the present time, because impact events are unlikely to have demagnetized the entire surface. Spectral features of the Vestan surface indicate that space weathering effects are more subdued than those observed on the Moon (*47*) and may require shielding from the solar wind ion flux at 2.36 astronomical units by a surface field ≥0.2 μT (*48*). The existence of >2-μT magnetic fields of the intensities estimated here are therefore sufficient to stand off solar wind ions at the orbital distance of Vesta, providing a possible explanation for the apparently limited effects of solar wind ion-generated space weathering.

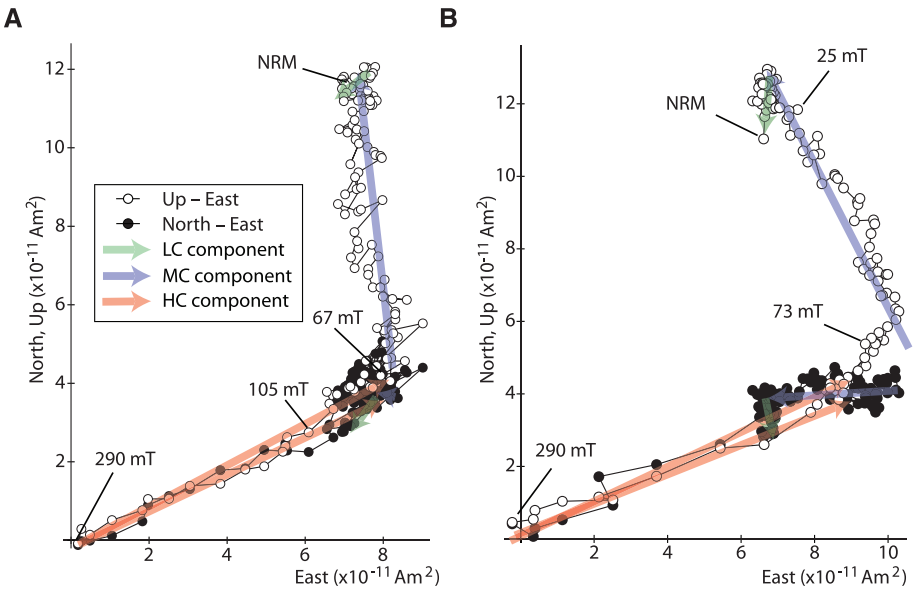

Fig. 2. Demagnetization of eucrite ALHA81001. Orthographic projections of the evolution of the NRM during AF demagnetization of two interior subsamples are shown. Open and solid circles indicate the projection of the NRM vector onto the vertical (up-east) and horizontal (north-east) planes, respectively. Red, blue, and green arrows denote HC, MC, and LC components, respectively. Selected AF levels are labeled. (**A**) AF demagnetization of interior subsample A5. (**B**) AF demagnetization of interior subsample A6. The similarity between the two demagnetization sequences indicates unidirectional magnetization.

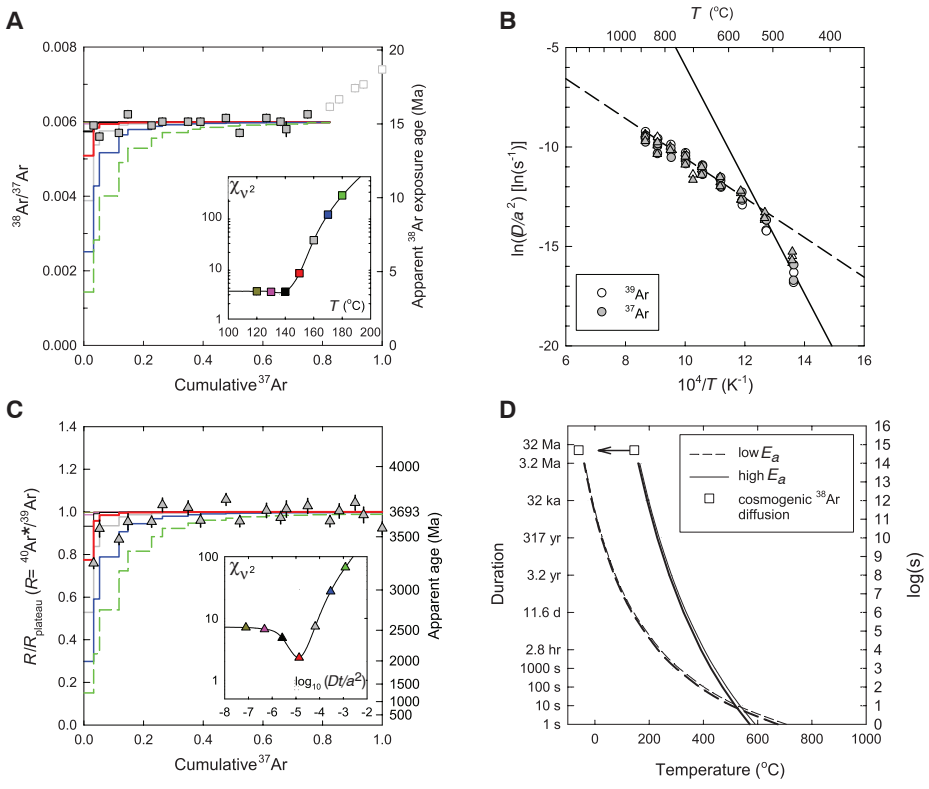

Fig. 3. ^{40}Ar and ^{38}Ar thermochronometry of ALHA81001. (**A**) Cosmogenic ^{38}Ar. Squares are observed ^{38}Ar/^{37}Ar ratios ±1 SD versus the release fraction of ^{37}Ar. Colored steps are synthetic release spectra calculated for the production and diffusion of cosmogenic ^{38}Ar over the apparent exposure duration of 15 My, assuming the Ar diffusion kinetics with maximum activation energy (E_a) in (B) (solid line) and isothermal temperatures ranging from <120° to 180°C. The inset shows reduced chi-squared (χ^2) fit statistics of each model compared to solid points, identifying the best-fit temperatures to be ≤140°C. (**B**) Diffusivity as a function of temperature (T) calculated (*49*) from ^{37}Ar and ^{39}Ar released during the first 19 heating steps of two degassing experiments; points are diffusion coefficients (D) divided by the square of the effective domain radius (a). The solid line quantifies kinetics with the apparent E_a determined from regression to the initial four extractions of each experiment; the dashed line gives the apparent E_a determined from the subsequent 16 extractions. The difference in these values of E_a may be due to a change in a or a non-uniform spatial distribution of ^{37}Ar and ^{39}Ar (*43*). We take the values of E_a for the first four extractions and the subsequent extractions as upper and lower bounds on the true value. (**C**) Production and diffusion of radiogenic Ar (^{40}Ar*). Triangles are measured ^{40}Ar*/^{39}Ar ratios (R) normalized to the mean ratio of the apparent plateau ($R_{plateau}$) versus the cumulative ^{37}Ar release fractions. The colored steps are model release spectra for heating conditions, as in (A), normalized to a mean plateau age of 3.693 ± 0.071 Ga (±1 SD); the inset identifies log$_{10}$(Dt/a^2) = −5 as the best-fit solution, where t is the duration of heating. (**D**) Duration and temperature constraints on possible thermal excursions experienced by ALHA81001. Solid curves are upper bounds on permissible thermal events at 15 million years ago (Ma) (bold curve) and at 1.0 Ga (thin curve) that would best predict the observed ^{40}Ar*/^{39}Ar spectrum shown in (C), using the maximum apparent E_a in (B); dashed curves are calculated from models using the minimum apparent E_a in (B) for thermal events at 15 Ma (bold curve) and 1.0 Ga (thin curve). The squares are upper bounds from (A) for maximum and minimum values of E_a. Solar heating since ~15 Ma to mean effective temperatures between −50° and 140°C provides an internally consistent prediction of the entire Ar data set.

References and Notes

1. J. E. Chambers, *Earth Planet. Sci. Lett.* **223**, 241 (2004).
2. C. T. Russell *et al.*, *Science* **336**, 684 (2012).
3. R. P. Binzel, S. Xu, *Science* **260**, 186 (1993).
4. K. Righter, M. J. Drake, *Meteorit. Planet. Sci.* **32**, 929 (1997).
5. The beginning of the solar system here refers to 4.567 to 4.568 Ga, which corresponds to the formation of calcium-aluminum–rich inclusions, the first macroscopic solids in the solar system.
6. T. Kleine *et al.*, *Geochim. Cosmochim. Acta* **73**, 5150 (2009).
7. B. P. Weiss *et al.*, *Science* **322**, 713 (2008).
8. L. Carporzen *et al.*, *Proc. Natl. Acad. Sci. U.S.A.* **108**, 6386 (2011).
9. D. J. Stevenson, *Space Sci. Rev.* **152**, 651 (2010).
10. S. M. Cisowski, *Earth Planet. Sci. Lett.* **107**, 173 (1991).
11. See supplementary materials section 1.
12. D. W. Collinson, S. J. Morden, *Earth Planet. Sci. Lett.* **126**, 421 (1994).
13. B. P. Weiss, J. Gattacceca, S. Stanley, P. Rochette, U. R. Christensen, *Space Sci. Rev.* **152**, 341 (2010).
14. T. Nagata, *Mem. Natl. Inst. Polar Res. Spec. Issue* **17**, 233 (1980).
15. See supplementary materials sections 2.1 to 2.3.
16. E. R. D. Scott, R. C. Greenwood, I. Franchi, I. S. Sanders, *Geochim. Cosmochim. Acta* **73**, 5835 (2009).
17. See supplementary materials section 2.3.
18. D. Walker, M. A. Powell, G. E. Lofgren, J. F. Hays, *Proc. Lunar Planet Sci. Conf. 9th*, 1369 (1978).
19. T. L. Grove, *Am. Mineral.* **67**, 251 (1982).
20. Undulatory extinction is characterized by dark bands that roll across a crystal when the sample is rotated during crossed-polar transmitted light microscopy. It is due to the realignment of crystallographic axes by heavy shock.
21. A. Bischoff, D. Stoffler, *Eur. J. Mineral.* **4**, 707 (1992).
22. See supplementary materials section 3.5.
23. See supplementary materials section 3.3.
24. A. Stephenson, D. W. Collinson, *Earth Planet. Sci. Lett.* **23**, 220 (1974).
25. I. Garrick-Bethell, B. P. Weiss, *Earth Planet. Sci. Lett.* **294**, 1 (2010).
26. D. J. Dunlop, O. Ozdemir, D. A. Clark, P. W. Schmidt, *Earth Planet. Sci. Lett.* **176**, 107 (2000).
27. See supplementary materials section 3.4.
28. L. T. Elkins-Tanton, B. P. Weiss, M. T. Zuber, *Earth Planet. Sci. Lett.* **305**, 1 (2011).
29. M. G. Sterenborg, J. L. Crowley, in *43rd Lunar and Planetary Science Conference* (Houston, TX, 2012), abstr. 2361.
30. K. E. Haisch Jr., E. A. Lada, C. J. Lada, *Astrophys. J.* **553**, L153 (2001).
31. See supplementary materials section 4.4.
32. N. J. Turner, T. Sano, *Astrophys. J.* **679**, L131 (2008).
33. M. Miyamoto, H. Takeda, abstract in *57th Meeting of the Meteoritical Society* (Prague, 1994).
34. L. L. Hood, N. A. Artemieva, *Icarus* **193**, 485 (2008).
35. D. A. Crawford, P. H. Schultz, *Int. J. Impact Eng.* **23**, 169 (1999).
36. L. L. Hood, A. Vickery, *Proc. Lunar Planet. Sci. Conf. 15th*, C211 (1984).
37. E. Pierazzo, A. M. Vickery, H. J. Melosh, *Icarus* **127**, 408 (1997).
38. E. Asphaug, *Meteorit. Planet. Sci.* **32**, 965 (1997).
39. U. R. Christensen, J. Aubert, *Geophys. J. Int.* **166**, 97 (2006).
40. M. A. Wieczorek, B. P. Weiss, S. T. Stewart, *Science* **335**, 1212 (2012).
41. P. Rochette *et al.*, *Meteorit. Planet. Sci.* **44**, 405 (2009).
42. J. Gattacceca, P. Rochette, *Earth Planet. Sci. Lett.* **227**, 377 (2004).
43. See supplementary materials section 2.2.
44. V. Reddy *et al.*, *Science* **336**, 700 (2012).
45. R. C. Greenwood, I. A. Franchi, A. Jambon, J. A. Barrat, T. H. Burbine, *Science* **313**, 1763 (2006).
46. L. L. Hood, A. Zakharian, *J. Geophys. Res.* **106**, 14601 (2001).
47. M. C. De Sanctis *et al.*, *Science* **336**, 697 (2012).
48. P. Vernazza *et al.*, *Astron. Astrophys.* **451**, L43 (2006).
49. H. Fechtig, S. Kalbitzer, in *Potassium-Argon Dating*, O. A. Schaeffer, J. Zahringer, Eds. (Springer, Heidelberg, 1966), pp. 68–106.

Acknowledgments: We thank the Johnson Space Center staff and the Meteorite Working Group for allocating ALHA81001, A. Bevan at the Western Australia Museum for allocating Millbillillie, P. Rochette for helpful discussions, N. Chatterjee for help with the microprobe analyses, S. Chu for help with the MPMS-XL analyses, and B. Carbone for administrative help. D.L.S. thanks W. S. Cassata for helpful discussions and the Ann and Gordon Getty Foundation for support. B.P.W. thanks the NASA Origins Program and Thomas F. Peterson for support. R.R.F. thanks the NSF Graduate Research Fellowship program for support. B.P.W. and C.S. thank the NASA Lunar Science Institute for support. Paleomagnetic and thermochronology data are found in the supplementary materials.

Supplementary Materials

www.sciencemag.org/cgi/content/full/338/6104/238/DC1
Supplementary Text
Figs. S1 to S19
Tables S1 to S7
References (*50*–*121*)
Database S1

5 June 2012; accepted 12 September 2012
10.1126/science.1225648